Eur Biophys J (2006) 35: 170–180
DOI 10.1007/s00249-005-0018-6

ARTICLE

Markus Zweckstetter

Prediction of charge-induced molecular alignment: residual dipolar couplings at pH 3 and alignment in surfactant liquid crystalline phases

Received: 27 May 2005 / Revised: 22 August 2005 / Accepted: 25 August 2005 / Published online: 26 October 2005

Abstract Recently we reported that the alignment tensor of a biological macromolecule, which was dissolved in a dilute suspension of highly negatively charged filamentous phage at close to neutral pH, can be predicted from the molecule's 3D charge distribution and shape (Zweckstetter et al. 2004). Here it is demonstrated that this approach is also applicable to alignment of proteins in liquid crystalline phases formed by filamentous phage at low pH. Residual dipolar couplings (RDCs) predicted by our simple electrostatic model for the B1 domain of protein G in fd phage at pH 3 fit very well with the experimental values. The sign of charge–shape predicted one-bond ^{1}H–^{15}N dipolar couplings for the B1 domain of protein G (GB1) was inverted at pH 3 compared to neutral pH, in agreement with experimental observations. Our predictions indicate that this is a feature specific for GB1. In addition, it is shown that RDCs induced in the protein ubiquitin by the presence of a positively charged surfactant system comprising cetylpyridinium bromide/hexanol/sodium bromide can be predicted accurately by a simple electrostatic alignment model. This shows that steric and electrostatic interactions dominate weak alignment of biomolecules for a wide range of pH values both in filamentous phage and in surfactant liquid crystalline phases.

Keywords Molecular alignment · Residual dipolar coupling · Liquid crystal · Electrostatics · NMR · Cetylpyridinium bromide · Surfactant · CHARMM

M. Zweckstetter
Department of NMR–based Structural Biology, Max Planck Institute for Biophysical Chemistry, Am Fassberg 11, 37077 Göttingen, Germany
E-mail: mzwecks@gwdg.de
Tel.: +49-551-2012220
Fax: +49-551-2012202

Introduction

Residual dipolar couplings (RDCs) can be measured in a weakly aligned macromolecule, for which the large one-bond internuclear dipolar interactions no longer average to zero (Tjandra and Bax 1997; Tolman et al. 1995). RDCs are exquisitely sensitive to bond vector orientation and offer many new opportunities in NMR studies of proteins in solution, ranging from structure validation and rapid structure determination to the study of dynamics (Cornilescu et al. 1998; Delaglio et al. 2000; Hus et al. 2001; Jung et al. 2004; Meiler et al. 2001, 2003; Tolman 2002). The partial alignment of the biomolecule in solution is usually accomplished by means of a dilute liquid crystalline medium or an anisotropically compressed gel (Barrientos et al. 2000; Clore et al. 1998; Fleming et al. 2000; Gabriel et al. 2002; Hansen et al. 1998; Meier et al. 2002; Prestegard et al. 2004; Prosser et al. 1998; Ruckert and Otting 2000; Sass et al. 1999; Tjandra and Bax 1997; Tycko et al. 2000).

Recently, we and others reported that RDCs observed for proteins and nucleic acids dissolved in dilute suspensions of the highly negatively charged filamentous phages at close to neutral pH can be predicted from the molecular shape and charge distribution (Ferrarini 2003; Zweckstetter et al. 2004). An highly oversimplified model, which approximated the electrostatic interaction between a solute and an ordered phage particle as that between the solute surface charges and the electric field of the phage, predicted both the magnitude and orientation of the solute's alignment tensor with reasonable accuracy (Zweckstetter et al. 2004). This electrostatic model extended an earlier approach that considered only steric obstruction (Zweckstetter and Bax 2000). The ability to predict dipolar couplings for a given protein structure provides possibilities for the differentiation between monomeric and homodimeric states (Zweckstetter and Bax 2000), conformational analysis of dynamic systems such as oligosaccharides (Azurmendi and Bush 2002), refinement of nucleic acid structures

(Warren and Moore 2001), determination of the relative orientation of protein domains (Bewley and Clore 2000), validation of structures of protein complexes (Bewley 2001) and classification of protein-fold families on the basis of unassigned NMR data (Valafar and Prestegard 2003). The electrostatic alignment model offers additional unique opportunities, such as the distinction between different relative conformations (e.g. parallel versus antiparallel) of a homodimeric system, that are not easily distinguished by steric alignment or other methods (Zweckstetter et al. 2005).

Besides the popular filamentous phage, many other charged media have been developed for alignment of biomolecules (Barrientos et al. 2000; Gabriel et al. 2002; Meier et al. 2002; Prestegard et al. 2004; Prosser et al. 1998; Ramirez and Bax 1998; Sass et al. 1999). Different alignment media are important to obtain independent sets of RDCs for improved structure determination (Al-Hashimi et al. 2000). In addition, not all proteins are compatible with filamentous phage due to strong electrostatic or hydrophobic interactions. A good complement to the highly negatively charged phage medium is the quasi-ternary surfactant system comprising cetylpyridinium bromide (CPBR)/hexanol/sodium bromide. It is positively charged and allows partial alignment of macromolecules at low pH (Barrientos et al. 2000). NMR measurements below pH 4 are, for example, important for protein-folding studies. If the protein is partially unfolded under these conditions, NOE-based methods for structure determination are only of limited use due to the highly dynamic nature of the system, making RDCs particularly important for structure determination (Mohana-Borges et al. 2004).

Here, it is shown that RDCs measured in lamellar phases formed by CPBR/hexanol/salt mixtures can be predicted by our simple electrostatic alignment model. In addition, RDCs that were predicted assuming a fully protonated B1 domain of protein G are in very good agreement with values measured at pH 3 in fd filamentous phage. A purely steric alignment model, on the other hand, was not sufficient to explain RDCs at pH 3. This demonstrates that it is not only possible to predict alignment of biomolecules dissolved at close to neutral pH in the nematic phase of rod-shaped filamentous phage, but that our simple electrostatic model is also applicable to partial alignment at low pH and in surfactant liquid crystalline systems.

Materials and methods

Experimental residual dipolar couplings

Experimental residual ^{15}N–^{1}H dipolar couplings used in this study were measured by different laboratories (Barrientos et al. 2001; Peti et al. 2002; Ulmer et al. 2003). In brief, $^{1}D_{NH}$ couplings for the 56-residue first Igg-binding domain of protein G (further referred to as GB1) at pH 8.0 were measured in 30 mg/ml fd filamentous phage in 10 mM Tris–HCl buffer, 90% H_2O/10% D_2O. For RDC measurements at pH 3.0 a 10 mM sodium citrate buffer was used (Barrientos et al. 2001). $^{1}D_{NH}$ couplings in the 56-residue third Igg-binding domain of protein G (further referred to as GB3) at pH 6.5 were measured in 11 mg/ml Pf1 bacteriophage (ASLA, Ltd, Latvia), 100 mM NaCl, 25 mM NaH_2PO_4/Na_2HPO_4 (Ulmer et al. 2003). $^{1}D_{NH}$ couplings for the 76-residue protein ubiquitin were measured in 5 mg/ml Pf1 bacteriophage (ASLA, Ltd), 50 mM NaCl, 10 mM NaH_2PO_4/Na_2HPO_4, pH 6.5, as well as in the lamellar phase formed by 5% cetylpyridinium bromide/hexanol (1.33/1; w/w) in 25 mM NaBr, 90% H_2O/10% D_2O, pH 6.5 (Peti et al. 2002).

Coordinates

In our calculations high-resolution NMR structures of GB1 (PDB code: 3GB1) and ubiquitin (PDB code: 1D3Z; mean structure), which were determined at close to neutral pH, were used (Cornilescu et al. 1998; Kuszewski et al. 1999). The coordinates of hydrogen atoms of 3GB1 were recalculated with XPLOR-NIH (Schwieters et al. 2003). For GB3 no high-resolution NMR structure (including side chains), determined with a large number of NOEs and RDCs, is available. For the 1.1 Å X-ray structure of GB3 (PDB code: 1IGD), on the other hand, a lower correlation between charge-shape-predicted RDCs and experimental values (measured at pH 7.0 in Pf1 bacteriophage) was observed, as was expected based on the very high resolution of this structure. The lower prediction quality was attributed to partially altered orientations of the titratable groups in the crystalline compared to the solution state (Zweckstetter et al. 2004). Therefore, an ensemble of 100 GB3 models was generated by keeping the backbone of the X-ray structure fixed while subjecting all side chains to a brief low-temperature-simulated annealing run using the structure calculation program XPLOR-NIH. This resulted in structures that deviate by less than 0.95 Å for all non-H atoms. Molecular alignment predictions employing the rod-shaped alignment model were performed for all 100 structures at pH 6.5 and pH 3.0.

Models for liquid crystal particles

Pf1 and fd filamentous bacteriophages are semiflexible (wormlike) polyelectrolytes 6.6 nm in diameter (Liu and Day 1994). The virion comprises a coat of several thousand identical protein subunits in a helical array surrounding a DNA core, with a few minor proteins capping the two ends of the virion. The ionic properties of filamentous phage are completely determined by the titrating groups in the amino terminal half of the coat protein. These groups are on the surface of the virus particle. Three aspartic acids and the terminal amino group contribute to the ionic properties of Pf1 phage. In

fd, three aspartic acids, two glutamic acids, one lysine and the terminal amino group are important (Zimmermann et al. 1986).

In the calculations, the virion is modelled as an infinite cylinder with uniform surface charge density. The simulation parameters were essentially as described before, with a cylinder radius of 3.35 nm, density of 1.46 g/cm^3 and a liquid crystal order parameter of 0.9 for both fd and Pf1 bacteriophage (Zweckstetter et al. 2004). The static dielectric constant of water was 78.29. To evaluate steric clash between the solute and the liquid crystal particle, radii of solute atoms were set to zero. For simulations at close to neutral pH the surface charge density was set to -0.475 e/nm^2. At pH 3.0 filamentous phage is highly positively charged and the surface charge density was set to $+0.475$ e/nm^2 (Zimmermann et al. 1986). All other simulation parameters were the same at low and high pHs.

The lamellar phase of CPBR/hexanol/sodium bromide was modelled as a uniformly charged wall, with a thickness of 26.8 Å and a liquid crystal order parameter of 0.8. The surface charge density was set to $+0.08$ e/nm^2 (see Results and discussion for further details).

Charges on proteins

We considered as titratable groups the C-terminus, the N-terminus and all aspartates, glutamates, arginines, lysines and histidines. Two different charge models were tested. In the first model the protein was represented by the charges of its ionizable residues and no atomic partial charges were included. At close to neutral pH all ionizable residues, except for histidine, were assumed to be fully charged (charge of 1.0e for Arg and Lys, -1.0e for Glu and Asp). The N- and C-termini also carried charges of 1.0e and -1.0e, respectively. At pH 3.0 only Arg, Lys and the N-terminus carry a charge of 1.0e. The protonation state of His68 in ubiquitin was calculated using the Henderson–Hasselbach equation, assuming a reference pKa of 6.3 (charge of 0.33e at pH 7; Antosiewicz et al. 1994). Charges were distributed evenly over the heavy atoms involved (e.g. both N^{η} atoms for Arg, but only N^{ζ} for Lys).

For the more detailed model, atomic partial charges from the CHARMM22 force field were included (Mackerell et al. 1992). Opposite to the CHARMM22 force field, however, the proton of protonated carboxyl groups was not represented explicitly, but simply by symmetrically distributing its charge to the atoms of the unprotonated carboxyl group. This was done because the exact binding site of the proton is not known. It was demonstrated in the past that this simplification works properly (Rabenstein and Knapp 2001). For similar reasons, the deprotonation of Arg, Lys and the N-terminus was represented by symmetrically removing a unit positive charge from the atoms of the titratable group. The charges of deprotonated tyrosine, which are not part of the CHARMM22 parameter set, were set based on quantum chemical calculations (Rabenstein et al. 1998). The influence of water was not considered. Atomic partial charges that are not explicitly part of the CHARMM22 parameter set are listed in Table 1.

The electrostatic alignment model, as implemented in the dipolar coupling analysis software PALES (M. Zweckstetter, unpublished; PALES is available upon request from mzwecks@gwdg.de), was used for the prediction of charge-induced RDCs. The CHARMM22 charge model was implemented and can be accessed by calling PALES with the '*-charmm22*' command line argument. The protonation state of titratable groups is based on the pH value ('*-pH*' command line argument). The alignment model in which the liquid crystal particle is represented by an infinite wall can be accessed using the '*-wall*' command line argument.

Accuracy of charge-shape prediction

To evaluate the accuracy of charge–shape prediction, experimental RDCs were compared with charge-shape-predicted values using Pearson's linear correlation coefficient R_P. In this comparison only those experimental RDCs were included that can be best-fit almost perfectly (correlation between experimental and best-fitted RDCs >0.99) to the backbone of the reference structures using singular value decomposition as implemented in the program PALES.

Theory

In our electrostatic alignment model, the nematogen is approximated by an infinite wall (CPBR/hexanol/NaBr) or infinite cylinder (filamentous phage), oriented parallel to the magnetic field (z-axis). The centre of gravity of the

Table 1 Atomic partial charges of titratable groups

Group	Protonated	Deprotonated
Carboxyl (except C-term)		
C-α	−0.21	−0.28
Carboxyl C	0.75	0.62
Carboxyl O (2×)	−0.36	−0.76
C-terminus		
Carboxyl C	0.34	0.34
Carboxyl O (2×)	−0.17	−0.67
Arginine		
N-ε	−0.70	−0.81
C-ζ	0.64	0.71
Guanidino N (2×)	−0.80	−0.90
Guanidino H (4×)	0.46	0.27
Lysine/N-terminus		
Amino N	−0.30	−0.97
Amino H (3x)	0.33	0.22
Tyrosine		
C-ζ	0.11	−0.18
Hydroxyl O	−0.54	−0.82
Hydroxyl H	0.43	0.00

solute is moved on a 1D grid away from the surface of the liquid crystal model. At each step, a large number of different molecular orientations are sampled. For each orientation the program evaluates whether the solute sterically clashes with the nematogen, i.e. if any of the solute atoms has a coordinate within the wall or cylinder model. If this is not the case an alignment matrix A is calculated:

$$A_{ij} = \frac{1}{2}(3\cos\theta_i\cos\theta_j - \delta_{ij}) \quad (i, j = x, y, z) \tag{1}$$

where θ_i indicates the angle between the ith molecular axis and the z axis (magnetic field direction) and δ_{ij} the Kronecker delta. Using periodic boundary conditions, sampling is restricted to distances r between the solute centre of gravity and the centre of the bilayer or cylinder for which $r < d/(2V_f)$ (wall model) or $r < d/(4V_f)^{1/2}$ (cylinder), where d is either the wall thickness or the cylinder diameter and V_f the nematogen volume fraction.

Each sterically allowed orientation and distance is weighted according to the electrostatic interaction between the solute and the nematogen. The electrostatic interaction energy is calculated using continuum electrostatic theory (Debye and Hueckel 1923). Even within the simplifications of a continuum description, calculation of the electrostatic potential would require solving a full 3D electrostatics problem for each distance and orientation of the solute with respect to the surface of the charged liquid crystal particle. Instead, the problem is further simplified by treating the solute as a particle in the external field of the liquid crystal. Moreover, we assume the nematogen to carry a homogeneous surface charge density σ instead of discrete charges. The non-linear 3D Poisson–Boltzmann (PB) equation is then solved only once, in the absence of the solute, yielding an electrostatic potential $\phi(r)$. For a flat surface, an analytical solution of the non-linear PB equation for symmetric monovalent ions exists (Chapman 1913; Gouy 1910):

$$\frac{e\phi(x)}{k_B T} = 4\tanh^{-1}\left\{\tanh\left[\frac{1}{2}\sinh^{-1}\left(\frac{\sigma\kappa_D}{4\rho e}\right)\right]e^{-\kappa_D x}\right\}, \tag{2}$$

where the inverse Debye length κ_D is given by

$$\kappa_D = \frac{8\pi e^2\rho}{\varepsilon k_B T}, \tag{3}$$

where k_B is the Boltzmann factor, T the temperature, ρ the number density of ions in bulk solution ($\rho_+ = \rho_- = \rho$) and ε the static dielectric constant of the solvent. For uniformly charged cylinders (filamentous phage) the non-linear PB equation was solved with the method of Stigter (1982) assuming symmetric monovalent ions and vanishing potential at infinity.

The distance and orientation-dependent electrostatic free energy of the protein comprising partial charges q_i at positions r_i is then approximated by

$$\Delta G_{el}(r, \Omega) = \sum_i q_i \phi[r_i(r, \Omega)]. \tag{4}$$

The Boltzmann factor $p_B = \exp[-\Delta G_{el}(r, \Omega)/k_B T]$ provides relative electrostatic weights when averaging the individual alignment tensors, derived for each orientation and distance (Eq. 1), to yield an overall solute alignment tensor

$$A_{ij}^{mol} = \frac{\int A_{ij} p_B(r, \Omega)\mathrm{d}r\mathrm{d}\Omega}{\int p_B(r, \Omega)\mathrm{d}r\mathrm{d}\Omega}. \tag{5}$$

The imperfect alignment of liquid crystals is taken into account by multiplication of A^{mol} with the order parameter of the liquid crystal.

Results and discussion

Charge-shape prediction of RDCs at pH 3

Prediction of molecular alignment at pH 3 was investigated for the 56-residue first Igg-binding domain of protein G (GB1). GB1 is very rigid, and a high-resolution NMR structure is available (Fig. 1a), providing excellent conditions for prediction of alignment from structure. GB1 comprises five aspartates, five glutamates and six lysines such that 11 negative and 7 positive charges are present at close to neutral pH. The distribution of these charges on the surface results in a dipole moment of ~81 Debye and a quadrupole moment of $\sim 1.8\times10^3$ Å^2 e at pH 7.0 (Fig. 1b and Table 2). Despite the very high resolution of the NMR structure with a coordinate rmsd of 1.0 Å for all non-H atoms, there are significant variations in the position of the titratable groups across the ensemble of 32 structures, which is available from the ProteinDataBank. Due to these variations the calculated dipole and quadrupole moment vary from 48 to 112 Debye and from 1.5×10^3 Å^2 e to 2.2×10^3 Å^2 e, respectively (not taking into account atomic partial charges; Table 2). At pH 3.0, GB1 (pI = 4.5) is assumed to be fully protonated resulting in a highly positively charged protein with a net charge of +7 e and a quadrupole moment of $\sim 2.4\times10^3$ Å^2 e (Fig. 1c and Table 2).

Figure 2a compares experimental ^{1}H–^{15}N RDCs measured for GB1 in fd filamentous phage at pH 8.0 with values predicted from our simple electrostatic model on the basis of GB1's shape and charge distribution. A very good agreement between experimental and charge-shape-predicted values was obtained, indicating that RDCs measured in highly negatively charged filamentous phage at close to neutral pH can be predicted accurately by our alignment model (Fig. 2a). At pH 3 the electrostatics of the system are strongly altered with a positive surface charge of filamentous phage (isoelectric point of pH 4.2 for fd phage) and a purely positively charged GB1 protein. For these conditions the maximum correlation between charge-shape-predicted

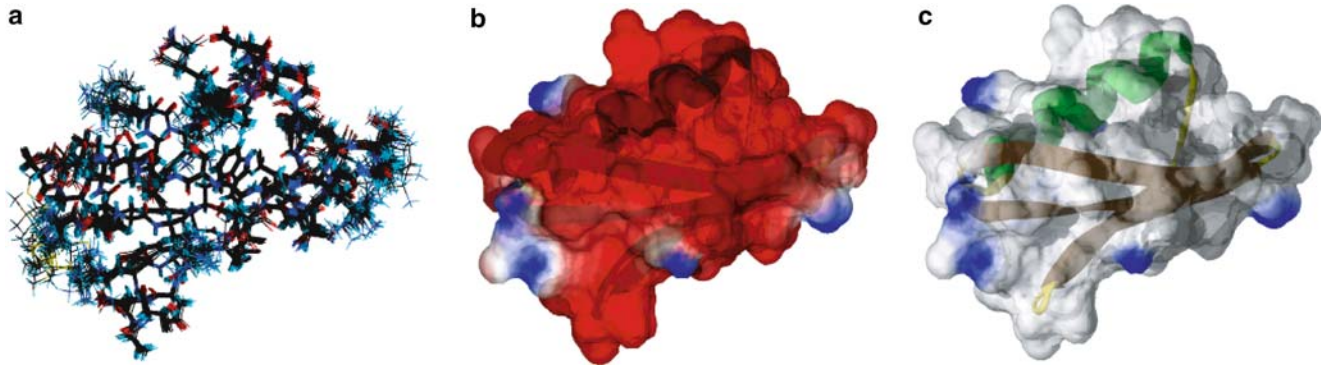

Fig. 1 Three-dimensional structure of the B1 domain of protein G (PDB code: 3GB1). **a** Ensemble of high-resolution NMR structures highlighting the variation in side chain orientations within the ensemble of 32 structures. **b** Electrostatic surface model at neutral pH with positive and negative potentials coloured *blue* and *red*, respectively. **c** Electrostatic surface model at pH 3 [generated using the program SwissPdb Viewer (Guex and Peitsch 1997)]

RDCs and experimental values across the ensemble of GB1 structures was 0.91 (Fig. 2b). Despite the fact that only seven positively charged groups are present at pH 3, R_p values varied significantly for different members of the ensemble of NMR structures, ranging from 0.59 to 0.91 (Table 3). This variation is slightly less than that at pH 8.0, at which R_p values ranged from 0.53 to 0.98, in agreement with the lower number of charged groups.

When electrostatic interactions were switched off in the simulations and only steric obstruction was considered, the maximum correlations between predicted and experimental RDCs were 0.61 and −0.53 at pH 3.0 and pH 8.0, respectively (Table 3). At low pH both the anisotropic medium and the protein carry positive charge and the alignment is dominated by repulsive forces. Although such alignment is more in agreement with a purely steric model than that at close to neutral pH, at which alignment is the result of a delicate balance between attractive and repelling forces, a steric model is not sufficient to explain RDCs at pH 3.0. Due to the non-uniform distribution of positive charges on the surface of GB1, orientations of the protein, in which more positive charges come close to the virion's surface, are less favourable.

The maximum as well as the average correlation between charge-shape-predicted RDCs and experimental values was significantly lower at pH 3.0 [R_P(max) = 0.91; R_P(mean) = 0.80] than at pH 8.0 [R_P(max) = 0.98; R_P(mean) = 0.85] (Table 3). At low pH the helical symmetry of the protein coat of fd phage changes compared to pH 8 due to the altered surface charge. The very high quality of alignment prediction at pH 8, however, indicates that structural details of the virus particle are less important and alignment of GB1 is dominated by long-range electrostatic interaction. Therefore, the changes in helical symmetry of fd are unlikely to play a significant role. In addition, no conformational changes of the backbone occur for GB1 even at pH 3, as evidenced by the quality of a best-fit of experimental RDCs at pH 3 to the NMR structure (determined at close to neural pH) using singular value decomposition [R_P(SVD) > 0.98]. Thus, the lower correlation between charge-shape-predicted RDCs and experimental values suggests that, although the backbone of GB1 is not changed, the orientation of positively charged groups is partially altered when the pH is decreased from 8 to 3. Note, however, that it cannot be excluded that the influence of other interactions becomes important at low pH, at which there is no strong elec-

Table 2 Multipole moments of GB1 at pH 3.0 and pH 8.0 calculated for the ensemble of NMR structures (PDB code: 3GB1)

Multipole	Mean	rmsd	Minimum	Maximum
pH 3.0				
Monopole [e]	+7.0	–	–	–
Dipole [Debye]	0	–	–	–
Quadruple [10^3 Å^2 e] [a]	2.4	0.2	2.0	2.6
pH 8.0				
Monopole [e]	−4.0	–	–	–
Dipole [Debye]	81	17	48	112
Quadruple [10^3 Å^2 e][a]	1.8	0.2	1.5	2.2

[a]The magnitude of the quadrupole moment, GMag(Quad), is calculated after diagonalization of the symmetric, traceless quadrupole tensor using GMag(Quad) = $2Q_a\,[\pi(4 + 3(Q_r/Q_a)^2)/5]^{1/2}$, where Q_a and Q_r are the axial and rhombic components of the quadrupole tensor

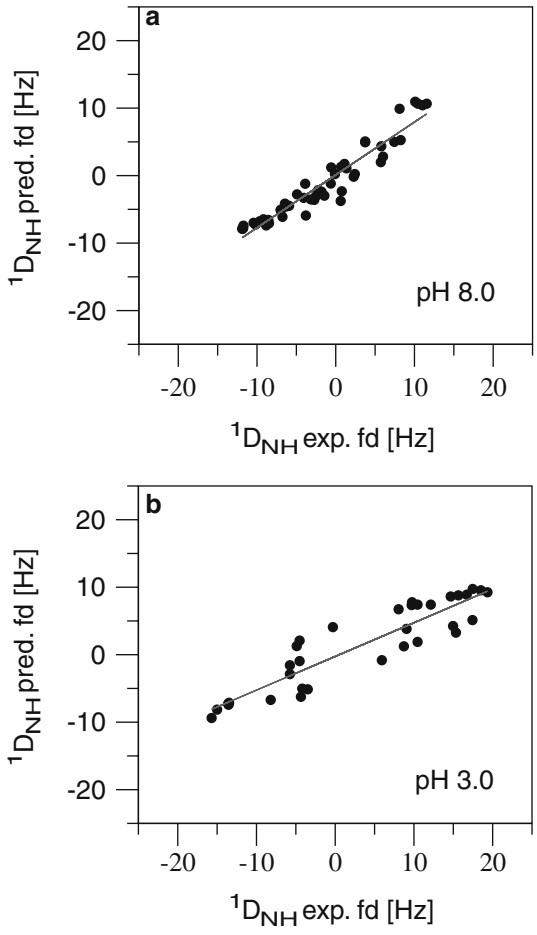

Fig. 2 Residual dipolar couplings for GB1 in fd phage at pH 3. **a** Comparison of experimental $^1D_{NH}$ couplings for GB1 in fd (~30 mg/ml; in 10 mM Tris–HCl buffer, pH 8.0) with values predicted on the basis of GB1's 3D shape and charge distribution ($^1D_{NH}$ *pred.*) at neutral pH. The correlation coefficient is 0.96. **b** Comparison of experimental $^1D_{NH}$ couplings for GB1 in ~30 mg/ml fd, 10 mM sodium citrate buffer, pH 3.0, with values predicted on the basis of GB1's 3D shape and charge distribution. The correlation coefficient is 0.91. For details regarding the simulation of charge-shape-predicted RDCs, see text

trostatic attraction between opposite charges on the protein and the liquid crystal particle or, in general, that under these conditions our alignment model approximates the alignment of biomolecules less accurately.

The magnitude of alignment that is predicted at pH 3 underestimates the experimental value by a factor of about two (Fig. 2b). Our previous studies on molecular alignment in Pf1 phage at pH 7 showed that repulsion (attraction) of molecules with a net negative (positive) charge from the negatively charged virion is overestimated by our simple model particularly at low ionic strengths (below 150 mM NaCl). Thus, for GB1 in the fd alignment medium at pH 3, when both the virus particle and the protein are positively charged, the underestimation of the alignment magnitude might be due to the shortcomings of our simple electrostatic model. In addition, the predicted alignment magnitude depends strongly on the value of the surface charge density used in the calculations (data not shown).

Improved prediction quality with atomic partial charges

In our previous studies inclusion of atomic partial charges according to the CHARMM TOPH19 parameter set did not consistently improve the quality of charge-shape prediction at pH 7 in Pf1 phage for four tested proteins (ubiquitin, DinI, GB3 and GB1). Other factors, in particular the quality of the structure (for GB3 and GB1), the conformation of any flexible tails (for ubiquitin) and the exact charge that was put on histidines (for ubiquitin and DinI), had a more pronounced effect on the quality of prediction. GB1 does not contain any histidine, is a very rigid protein without any flexible tails and, with the recently published NMR structure of GB1 that was refined with a large number of NOEs and RDCs, a highly accurate structure is also available. Therefore, we investigated if inclusion of atomic partial charges according to the CHARMM22 force field has a significant effect on the prediction of RDCs from the high-resolution NMR structure of GB1 (PDB code: 3GB1). The correlation factors between predicted and experimental RDCs for increasing detail of the simulation and at two different pH values in fd phage are shown in Table 3. If no atomic partial charges were included and only the titrating groups were charged, the minimum and maximum correlations observed for the ensemble of GB1 structures were 0.44 and 0.97 at pH 8.0 and 0.57 and 0.88 at pH 3.0, respectively. The predicted alignment tensors were virtually unchanged upon increasing the resolution of the orientational grid (Table 3). Inclusion of atomic partial charges from the CHARMM22 parameter set increased the maximum correlation to 0.98 and 0.91 at pH 8.0 and pH 3.0, respectively. In addition, fitting a straight line to a comparison of correlation factors obtained from the calculations without and with atomic partial charges for the ensemble of GB1 structures resulted in a correlation of 0.93, a slope of 0.64 and an offset of 0.36 at pH 8.0. The corresponding values were 0.95, 0.97 and 0.07 at pH 3.0 (data not shown). These data indicate that inclusion of atomic partial charges makes charge-shape prediction more stable against inaccuracies in the orientation of charged groups and slightly improves the quality of prediction.

Inversion of the sign of ^1H–^{15}N RDCs for GB1 at pH 3

Previously, it was reported that the sign of ^1H–^{15}N RDCs for GB1 in fd phage is inverted at pH 3 compared to high pH values (Fig. 3a; Barrientos et al. 2001). We were interested to see if the sign inversion is in agreement with our predictions and if it is a general property of the alignment of proteins at low pH. Figure 3b shows that RDCs are inverted at low pH in the charge-shape pre-

Table 3 Influence of the charge model on the correlation between experimental and charge-shape-predicted RDCs for the ensemble of GB1 structures (PDB code: 3GB1)

Charge model	R_P (mean)	R_P (rmsd)	R_P (minimum)	R_P (maximum)
pH 3.0				
Steric only[a]	0.48	0.04	0.38	0.61
Ionizable AA[b]	0.75	0.07	0.57	0.88
Ionizable AA, high resolution[c]	0.75	0.07	0.57	0.88
CHARMM22[d]	0.80	0.07	0.59	0.91
pH 8.0				
Steric only[a]	−0.59	0.04	−0.67	−0.53
Ionizable AA[b]	0.77	0.14	0.44	0.97
Ionizable AA, high resolution[c]	0.77	0.14	0.44	0.97
CHARMM22[d]	0.85	0.10	0.53	0.98

[a]No electrostatics were included, only steric obstruction was considered

[b]No atomic partial charges were included. GB1 was represented by the charges of its ionizable residues

[c]As in b, but with a higher resolution orientational sampling: the *z*-axis of the molecule sampled 362 instead of 122 points on a unit sphere and the rotation around the *z*-axis was done in 10° steps (instead of 20°)

[d]Atomic partial charges were taken from the CHARMM22 force field except for the modifications listed in Table 1

dictions. For other proteins, such as ubiquitin, ^{1}H–^{15}N RDCs at low and high pHs will not be anticorrelated according to our predictions (Fig. 4). Even for GB3 there was no correlation between RDCs at low and high pHs. Despite its high sequence similarity, GB3 differs from GB1 by only seven residues with one glutamate replaced by a lysine and a glutamate located at position 24 instead of position 42, the correlation factor between RDCs at pH 6.5 and pH 3.0 was −0.3 (Fig. 4b). Thus, inversion of ^{1}H–^{15}N RDCs at low pH compared to high pH is a very specific property of GB1. For proteins other than GB1, which are stable at low pH, this offers the possibility to obtain two independent sets of RDCs from a single medium by partial alignment at high and low pHs.

Prediction of the alignment in cetylpyridinium bromide/hexanol/sodium bromide

Quasi-ternary systems of surfactant/alcohol/salt form lamellar phases that are stabilized by electrostatic repulsion and entropic effects. These phases consist of bilayers, which can be swollen by solvent, such that the spacing between bilayers is much larger than the thickness of the bilayer (Fig. 5; Helfrich 1978). It was shown that cetylpyridinium chloride and cetylpyridinium bromide/hexanol/salt mixtures allow the partial alignment of biological macromolecules (Barrientos et al. 2000; Prosser et al. 1998). Six percent CPBR/hexanol/NaBr form a very regular α-lamellar phase, in which the bilayers have a thickness of ~3 nm with large interlamellar spacings (McGrath 1997).

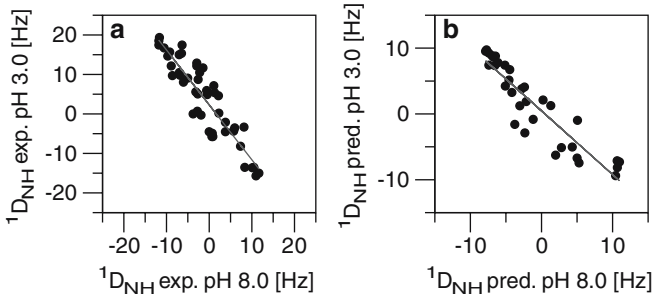

Fig. 3 Correlation between ^{1}H–^{15}N dipolar couplings for GB1 in the nematic phase of fd phage at different pH values. **a** Correlation between experimental RDCs at pH 8.0 and pH 3.0. The correlation coefficient is −0.91. **b** Correlation between charge-shape-predicted values at pH 8.0 and pH 3.0. The correlation coefficient is −0.92

Prediction of RDCs in CPBR/hexanol/NaBr was tested for the 76-residue protein ubiquitin. The CPBR/hexanol/NaBr liquid crystal matrix was modelled as a positively charged, infinite wall and the electrostatic potential was calculated from the analytical solution of the non-linear PB equation. The flat wall potential is very similar to that calculated for an infinite cylinder (Fig. 6). Figure 7 compares ^{1}H–^{15}N RDCs predicted for ubiquitin from the electrostatic flat wall model with experimental values measured in the lamellar phase formed by 5% CPBR/hexanol (1.33/1; w/w) in 25 mM NaBr at pH 6.5. The values are in very good agreement with a correlation factor of 0.94. When electrostatic interactions were not included and only steric obstruction was taken into account the correlation was 0.44. Thus, it is possible to predict RDCs in proteins that have been dissolved in a lamellar phase formed by CPBR/hexanol/NaBr from a highly simplified, electrostatic model.

The RDCs shown in Fig. 7 were calculated with a liquid crystal order parameter of 0.8. The exact value of the liquid crystal order parameter of the CPBR/hexanol/NaBr system, which was used for the measurement of RDCs in ubiquitin, is not known. The liquid crystal order parameter of weakly aligned DMPC/DHPC bicelles is about 0.8 (Vold and Prosser 1996). NMR diffusion experiments indicated that alignment of CPBR liquid crystals might not be as perfect as for bicelles, especially when equilibration of alignment was not suf-

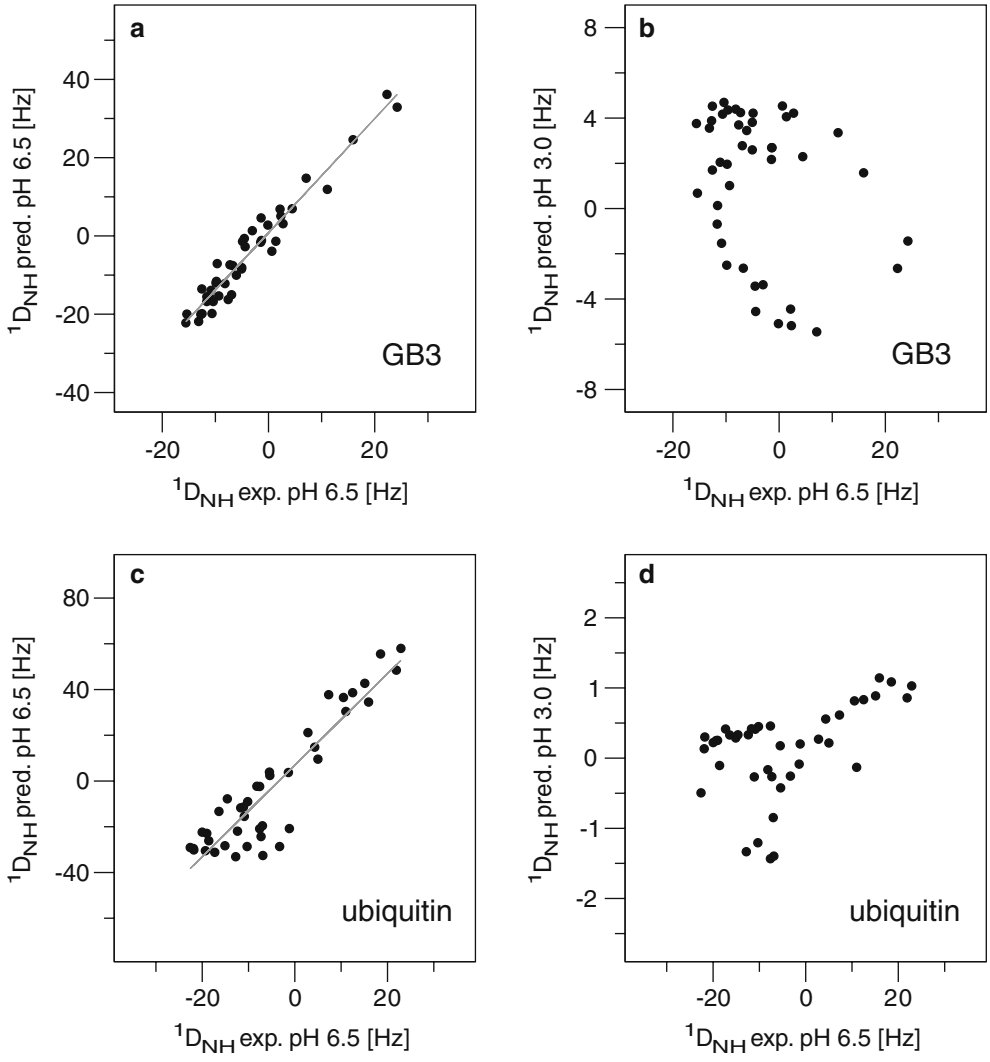

Fig. 4 Residual dipolar couplings for GB3 and ubiquitin in Pf1 phage at pH 6.5 and pH 3.0.
a Correlation between experimental and charge-shape-predicted ^1H–^{15}N RDCs for GB3, both at pH 6.5. Experimental values were measured in 11 mg/ml Pf1 bacteriophage, 100 mM NaCl, 25 mM NaH_2PO_4/Na_2HPO_4, pH 6.5. Predicted RDCs were calculated from the structure that gave the best prediction quality out of the ensemble of 100 calculated structures. The prediction quality for the ensemble of structures ranged from 0.54 to 0.97 and from 0.67 to 0.98 without or with atomic partial charges, respectively.
b Correlation between experimental $^1D_{NH}$ couplings for GB3 at pH 6.5 and charge-shape-predicted values at pH 3.0.
c Correlation between charge-shape-predicted and experimental ^1H–^{15}N RDCs for ubiquitin in Pf1 at pH 6.5. Experimental values were measured in 5 mg/ml Pf1, 50 mM NaCl, 10 mM NaH_2PO_4/Na_2HPO_4, pH 6.5.
d Correlation between experimental $^1D_{NH}$ couplings for ubiquitin at pH 6.5 and charge-shape-predicted values at pH 3.0. The correlation coefficients are 0.97 and 0.92 in **a** and **c**, respectively

ficiently long (Gaemers and Bax 2001). However, the influence of the exact value of the order parameter on the predicted magnitude of alignment is small compared to that of the average surface charge density of the CPBR liquid crystal. In the simulations a surface charge density of 0.08 e/nm^2 was assumed for the CPBR/hexanol/NaBr system. For lower values of the surface charge density the quality of charge-shape prediction was significantly worse with R_P values of 0.50, 0.59, 0.78 and 0.89 at 0.01, 0.02, 0.04, 0.06 e/nm^2, respectively. Higher surface charge densities strongly increased the predicted alignment magnitude, which was a factor of three higher at 0.15 e/nm^2 compared to that reported in Fig. 7. This suggests that the surface charge density of the CPBR/hexanol/NaBr liquid crystal, which was used for weak alignment of ubiquitin, had a surface charge density of about ~0.1 e/nm^2 at pH 6.5. A more accurate determination of the surface charge density is not possible, as the prediction of alignment magnitude using our simple electrostatic model is inaccurate, especially at low ionic strength (Zweckstetter et al. 2004).

There are several simplifications that enter our treatment of electrostatic effects. (1) Water and ions are treated at the continuum level, thus excluding the possibility of specific molecular interactions such as ion binding to the protein or the bilayer surface. (2) The

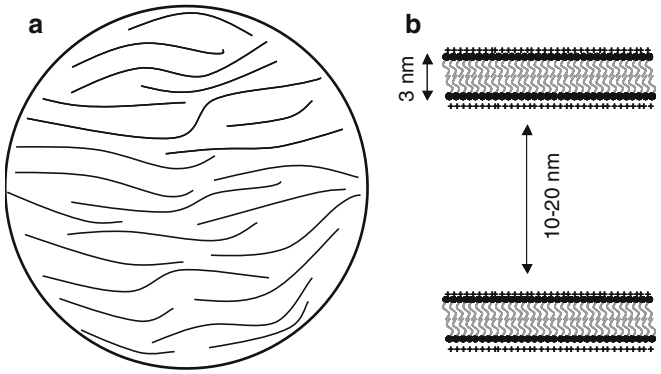

Fig. 5 Schematic representation of the cetylpyridinium bromide/hexanol/NaBr alignment system. **a** Morphology as seen from the top. A slice orthogonal to the NMR sample tube is depicted, which has its axis parallel to the magnetic field. **b** The lamellar phase consists of swollen bilayers with large interlamellar spacing (McGrath 1997)

orientation-dependent interactions of the protein with the charged interface are calculated using the electrostatic potential of the unperturbed interface. (3) The charge distribution on the liquid crystal particle is assumed to be uniform. (4) The protein structure and the charge distribution on the protein and interface are assumed to be rigid and independent of orientation and distance. In addition, non-polar interactions such as Born repulsion and non-polar attraction are neglected. However, the good agreement between experimental and charge-shape-predicted RDCs for ubiquitin suggests that short-range steric and long-range electrostatic effects dominate weak alignment of biomolecules in surfactant liquid crystalline systems. This is further supported by almost identical RDCs measured for

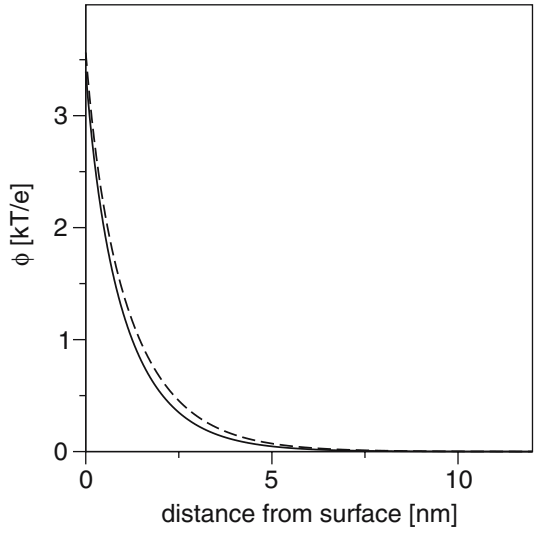

Fig. 6 Electrostatic potential of a flat surface calculated from the non-linear Poisson–Boltzmann equation. A homogeneous surface charge density of 0.47 e/nm^2 at 50 mM NaCl was used (*dashed line*). The electrostatic potential calculated for an infinite cylinder with a radius of 3.35 nm and a surface charge density of 0.47 e/nm^2 at 50 mM NaCl is included as *solid line*

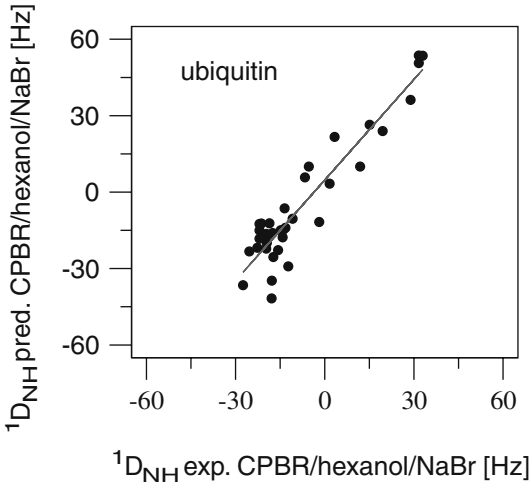

Fig. 7 Residual dipolar couplings for ubiquitin in positively charged surfactant systems. Comparison of $^1D_{NH}$ couplings predicted on the basis of ubiquitin's 3D shape and charge distribution with values measured for ubiquitin in the lamellar phase formed by 5% cetylpyridinium bromide/hexanol (1.33/1; w/w) in 25 mM NaBr, pH 6.5. The correlation coefficient is 0.94

GB1 at pH 3 in fd phage and in CPBR/hexanol/NaBr (Barrientos et al. 2001). A correlation of 0.994 between the two datasets strongly suggests that molecular details of the alignment medium besides the average surface charge density are not important for partial alignment of biological macromolecules.

In conclusion, it was shown that a simple electrostatic model can be used for the description of weak alignment of biological macromolecules at low pH and in surfactant liquid crystalline systems. RDCs observed in these conditions can be predicted accurately from the molecular shape and charge distribution, considering only short-range steric and long-range electrostatic interactions. Therefore, charge-shape prediction is likely to be equally applicable to many other dilute liquid crystalline media, which are currently used for weak alignment of proteins.

Acknowledgements The author thanks Laura G. Barrientos, Tobias S. Ulmer and Wolfgang Peti for making the RDCs of GB1, GB3 and ubiquitin available. This work was supported by the Max Planck Society. M.Z. is the recipient of a DFG Emmy Noether Fellowship (ZW71/1-4).

References

Al-Hashimi HM, Valafar H, Terrell M, Zartler ER, Eidsness MK, Prestegard JH (2000) Variation of molecular alignment as a means of resolving orientational ambiguities in protein structures from dipolar couplings. J Magn Reson 143:402–406

Antosiewicz J, Mccammon JA, Gilson MK (1994) Prediction of pH-dependent properties of proteins. J Mol Biol 238:415–436

Azurmendi HF, Bush CA (2002) Conformational studies of blood group A and blood group B oligosaccharides using NMR residual dipolar couplings. Carbohydr Res 337:905–915

Barrientos LG, Dolan C, Gronenborn AM (2000) Characterization of surfactant liquid crystal phases suitable for molecular

alignment and measurement of dipolar couplings. J Biomol NMR 16:329–337
Barrientos LG, Louis JM, Gronenborn AM (2001) Characterization of the cholesteric phase of filamentous bacteriophage fd for molecular alignment. J Magn Reson 149:154–158
Bewley CA (2001) Rapid validation of the overall structure of an internal domain-swapped mutant of the anti-HIV protein cyanovirin-N using residual dipolar couplings. J Am Chem Soc 123:1014–1015
Bewley CA, Clore GM (2000) Determination of the relative orientation of the two halves of the domain-swapped dimer of cyanovirin-N in solution using dipolar couplings and rigid body minimization. J Am Chem Soc 122:6009–6016
Chapman DL (1913) A contribution to the theory of electrocapillarity. Philos Mag 25:475–481
Clore GM, Starich MR, Gronenborn AM (1998) Measurement of residual dipolar couplings of macromolecules aligned in the nematic phase of a colloidal suspension of rod-shaped viruses. J Am Chem Soc 120:10571–10572
Cornilescu G, Marquardt JL, Ottiger M, Bax A (1998) Validation of protein structure from anisotropic carbonyl chemical shifts in a dilute liquid crystalline phase. J Am Chem Soc 120:6836–6837
Debye P, Hueckel E (1923) Zur Theorie der Elektrolyte. I. Gefrierpunktserniedrigung und verwandte Erscheinungen. Phys Zeitschr 24:185–206
Delaglio F, Kontaxis G, Bax A (2000) Protein structure determination using molecular fragment replacement and NMR dipolar couplings. J Am Chem Soc 122:2142–2143
Ferrarini A (2003) Modeling of macromolecular alignment in nematic virus suspensions. Application to the prediction of NMR residual dipolar couplings. J Phys Chem B 107:7923–7931
Fleming K, Gray D, Prasannan S, Matthews S (2000) Cellulose crystallites: a new and robust liquid crystalline medium for the measurement of residual dipolar couplings. J Am Chem Soc 122:5224–5225
Gabriel JCP, Camerel F, Lemaire BJ, Desvaux H, Davidson P, Batail P (2002) Swollen liquid-crystalline lamellar phase based on extended colloidal solid-like sheets: application for the structure determination f biomolecules using NMR. Abstr Pap Am Chem Soc 223:U394–U394
Gaemers S, Bax A (2001) Morphology of three lyotropic liquid crystalline biological NMR media studied by translational diffusion anisotropy. J Am Chem Soc 123:12343–12352
Gouy DL (1910) Sur la constitution de la charge électrique a la surface d'un électrolyte. Ann Phys 9:457–468
Guex N, Peitsch MC (1997) SWISS-MODEL and the Swiss-Pdb-Viewer: an environment for comparative protein modeling. Electrophoresis 18:2714–2723
Hansen MR, Mueller L, Pardi A (1998) Tunable alignment of macromolecules by filamentous phage yields dipolar coupling interactions. Nat Struct Biol 5:1065–1074
Helfrich W (1978) Steric interaction of fluid membranes in multilayer systems. Z Naturforsch A 33:305–315
Hus JC, Marion D, Blackledge M (2001) Determination of protein backbone structure using only residual dipolar couplings. J Am Chem Soc 123:1541–1542
Jung YS, Sharma M, Zweckstetter M (2004) Simultaneous assignment and structure determination of protein backbones by using NMR dipolar couplings. Angew Chem Int Ed 43:3479–3481
Kuszewski J, Gronenborn AM, Clore GM (1999) Improving the packing and accuracy of NMR structures with a pseudopotential for the radius of gyration. J Am Chem Soc 121:2337–2338
Liu DJ, Day LA (1994) Pf1 virus structure—helical coat protein and DNA with paraxial phosphates. Science 265:671–674
Mackerell AD, Bashford D, Bellott M, Dunbrack RL, Field MJ, Fischer S, Gao J, Guo H, Ha S, Joseph D, Kuchnir L, Kuczera K, Lau FTK, Mattos C, Michnick S, Nguyen DT, Ngo T, Prodhom B, Roux B, Schlenkrich M, Smith J, Stote R, Straub J, Wiorkiewiczkuczera J, Karplus M (1992) Self-consistent parameterization of biomolecules for molecular modeling and condensed phase simulations. FASEB J 6:A143–A143
McGrath KM (1997) Formation of two lamellar phases in the dilute region of a quasiternary surfactant system. Langmuir 13:1987–1995
Meier S, Haussinger D, Grzesiek S (2002) Charged acrylamide copolymer gels as media for weak alignment. J Biomol NMR 24:351–356
Meiler J, Prompers JJ, Peti W, Griesinger C, Bruschweiler R (2001) Model-free approach to the dynamic interpretation of residual dipolar couplings in globular proteins. J Am Chem Soc 123:6098–6107
Meiler J, Peti W, Griesinger C (2003) Dipolar couplings in multiple alignments suggest alpha helical motion in ubiquitin. J Am Chem Soc 125:8072–8073
Mohana-Borges R, Goto NK, Kroon GJA, Dyson HJ, Wright PE (2004) Structural characterization of unfolded states of apomyoglobin using residual dipolar couplings. J Mol Biol 340:1131–1142
Peti W, Meiler J, Bruschweiler R, Griesinger C (2002) Model-free analysis of protein backbone motion from residual dipolar couplings. J Am Chem Soc 124:5822–5833
Prestegard JH, Bougault CM, Kishore AI (2004) Residual dipolar couplings in structure determination of biomolecules. Chem Rev 104:3519–3540
Prosser RS, Losonczi JA, Shiyanovskaya IV (1998) Use of a novel aqueous liquid crystalline medium for high-resolution NMR of macromolecules in solution. J Am Chem Soc 120:11010–11011
Rabenstein B, Knapp EW (2001) Calculated pH-dependent population and protonation of carbon-monoxy-myoglobin conformers. Biophys J 80:1141–1150
Rabenstein B, Ullmann GM, Knapp EW (1998) Energetics of electron-transfer and protonation reactions of the quinones in the photosynthetic reaction center of Rhodopseudomonas viridis. Biochemistry 37:2488–2495
Ramirez BE, Bax A (1998) Modulation of the alignment tensor of macromolecules dissolved in a dilute liquid crystalline medium. J Am Chem Soc 120:9106–9107
Ruckert M, Otting G (2000) Alignment of biological macromolecules in novel nonionic liquid crystalline media for NMR experiments. J Am Chem Soc 122:7793–7797
Sass J, Cordier F, Hoffmann A, Cousin A, Omichinski JG, Lowen H, Grzesiek S (1999) Purple membrane induced alignment of biological macromolecules in the magnetic field. J Am Chem Soc 121:2047–2055
Schwieters CD, Kuszewski JJ, Tjandra N, Clore GM (2003) The Xplor-NIH NMR molecular structure determination package. J Magn Reson 160:65–73
Stigter D (1982) Mobility of water near charged interfaces. Adv Colloid Interface Sci 16:253–265
Tjandra N, Bax A (1997) Direct measurement of distances and angles in biomolecules by NMR in a dilute liquid crystalline medium. Science 278:1111–1114
Tolman JR (2002) A novel approach to the retrieval of structural and dynamic information from residual dipolar couplings using several oriented media in biomolecular NMR spectroscopy. J Am Chem Soc 124:12020–12030
Tolman JR, Flanagan JM, Kennedy MA, Prestegard JH (1995) Nuclear magnetic dipole interactions in field-oriented proteins - information for structure determination in solution. P Natl Acad Sci USA 92:9279–9283
Tycko R, Blanco FJ, Ishii Y (2000) Alignment of biopolymers in strained gels: a new way to create detectable dipole-dipole couplings in high-resolution biomolecular NMR. J Am Chem Soc 122:9340–9341
Ulmer TS, Ramirez BE, Delaglio F, Bax A (2003) Evaluation of backbone proton positions and dynamics in a small protein by liquid crystal NMR spectroscopy. J Am Chem Soc 125:9179–9191

Valafar H, Prestegard JH (2003) Rapid classification of a protein fold family using a statistical analysis of dipolar couplings. Bioinformatics 19:1549–1555

Vold RR, Prosser RS (1996) Magnetically oriented phospholipid bilayered micelles for structural studies of polypeptides. Does the ideal bicelle exist? J Magn Reson Ser B 113:267–271

Warren JJ, Moore PB (2001) Application of dipolar couplings to the refinement of the solution structure of the Sarcin-Ricin loop RNA. J Biomol NMR 20:311–323

Zimmermann K, Hagedorn H, Heuck CC, Hinrichsen M, Ludwig H (1986) The ionic properties of the filamentous bacteriophages Pf1 and Fd. J Biol Chem 261:1653–1655

Zweckstetter M, Bax A (2000) Prediction of sterically induced alignment in a dilute liquid crystalline phase: aid to protein structure determination by NMR. J Am Chem Soc 122:3791–3792

Zweckstetter M, Hummer G, Bax A (2004) Prediction of charge-induced molecular alignment of biomolecules dissolved in dilute liquid-crystalline phases. Biophys J 86:3444–3460

Zweckstetter M, Schnell JR, Chou JJ (2005) Determination of the packing mode of the coiled-coil domain of cGMP-dependent protein kinase I in solution using charge-predicted dipolar couplings. J Am Chem Soc 127(34):11918–11919